RSC Advances

ROYAL SOCIETY OF CHEMISTRY

www.rsc.org/advances

RSC Advances

RSCPublishing

ARTICLE

Cu hill and graphene grain evolution in a synthesis of millimeter-sized single crystal graphene during low pressure chemical vapor deposition‡

Cite this: DOI: 10.1039/xoxxoooooox

Received ooth January 2014,
Accepted ooth January 2014

DOI: 10.1039/xoxxoooooox

www.rsc.org/

Shuya Zhu, [†a] Quanfu Li, [†b] Qian Chen, [†a] Weihua Liu, [*b] Xin Li, [b] Juan Zhang, [b] Qikun Wang, [b] Xiaoli Wang [b] and Hongzhong Liu [*a]

The evolution of Cu hills beneath graphene grains during the growth of millimeter scale single crystal graphene using low pressure chemical vapor deposition (LPCVD) was investigated. We observed a Cu hill slope decreasing behavior as the graphene grain size increased. It indicated a hill self-flattening process under the growth temperature close to copper melting point. Especially the hill was almost completely flattened once the graphene grains merged. The evolution of the dendritic structure of the graphene grains was also studied. It was found that with a stepwise increased flow of CH_4, the interbranch boundaries in the dendritic structure can be healed. The blueshift of Raman 2D band as the Raman sampling spot moving from the grain center to the edge confirmed the improvement of the crystal quality due to the healing of the interbranch boundaries.

Introduction

Graphene, an atomically thin two dimensional carbon film, is of great interest owing to its novel physical properties and potential applications.[1] Of all the fabrication techniques, low pressure chemical vapor deposition (LPCVD) on Cu foils has been proven to be a promising route to prepare large area high quality and uniform graphene films.[2] The polycrystalline feature of the graphene film synthesized by LPCVD on copper foil is one of the main obstacles towards applications such as electronics[3] and flexible transparent conductive films[4]. To boost the graphene grain size is at present the subject of intense research in graphene synthesis. Most recently, the size of the single crystal graphene have been enlarged to wafer scale using CH_4 as carbon source.[5] Reduce the carbon source is one of the main strategies to suppress the nucleation and so increase the grain size.[5,6] However, at a low flow rate of carbon source, the growth rate is low and the growth time will be significantly elongated to hours.[5] One of the strategies is to use step-wise increased flow of carbon source as we do in this report.[7] Low flow of CH_4 is utilized at the initial stage to lower the graphene nucleation density. Then, the flow of CH_4 is increased to enhance the growth rate. It is also demonstrated that the higher the growth temperature used, the lower the graphene nucleation density and the larger the graphene grain size produced.[5b,5c,6c] To achieve millimeter scale sized graphene grains, the growth temperature is usually close to the melting point of copper. Long growth time with growth temperature close to the copper melting point is the common feature of the process condition for large scale graphene growth reported so far.[5,6,8]

In such a growth condition, if not intentionally making a sealed copper envelope to suppress the copper evaporation, copper foils will form hills beneath graphene grains, especially during LPCVD process.[9] Dendritic structures of graphene grains are also widely reported in such growth conditions.[5b,10] In this report, we focus on the evolution of Cu hills and the dendritic structure of graphene grains. For one thing is that the evaporation of Cu can lead to roughness especially during the long duration synthesis of large size single crystal graphene grains.[5b,10,11] It has been demonstrated that graphene grains preferentially nucleate on the evaporation-induced rough Cu surfaces and tends to replicate the substrate morphology.[5,6,8a,11,12] For another is that there are a lot of interbranch boundaries in the dendritic structure of graphene grains. Whether those interbranch boundaries can be healed is of particular interest for people who are exploring the possibility of connecting small graphene grains into a large one.

Experimental

Graphene growth

25-μm-thick Cu foils (99.8%, Alfa Aesar, #13382) were washed by 0.01M HCl for few seconds, followed by deionized (DI) water rinsing and N_2 blowing. The synthesis process was carried out in a 1-inch quartz tube furnace (Lindberg/Blue M, TF55035C-1, Thermo Electron Corp.). Cu foils were first annealed at 1077 ℃for 30 min under 100 sccm flow of Ar before the growth. Then Ar flow was shut off and then a mixture of H_2 and CH_4 was introduced into the chamber. The flow of H_2 was kept at 100 sccm for all of the growth process. Three growth experiments were carried out. The total growth time each of the three experiments is 3 hours. The flow rates of CH_4 in the three experiments are illustrated in Fig. 1a. The growth temperature was maintained at 1077 ℃ during the

whole process. Finally, CH_4 was turned off and the system was cooled to room temperature at a cooling rate of 50℃min^{-1} under protection of H_2.

Graphene transfer

After growth, the samples were spin-coated with a 300 nm thick polymethyl methacrylate (PMMA) layer (3000 r/min for 40s) and then baked on a hot plate at 120 ℃ for 5mins to cure the PMMA layer. Then, the graphene on the other side of the copper was removed by O_2 plasma exposure for 5mins. The Cu foil was etched with Marble's reagent for 90mins at 70 ℃. The graphene/PMMA film was rinsed by DI water it was picked up by target substrate (SiO_2/Si or TEM grid) and dried on hot plate at 80 ℃ for 10mins. Finally, the PMMA layer was removed in boiled acetone and it was followed by ethanol and DI water washing.

Characterization

Optical microscopy (VH-8000, KEYENCE), 3D measuring laser microscopy (LEXT OLS4000, OLYMPUS), SEM (Hitachi SU-8010), AFM (Innova, Veeco Instruments Inc.), TEM and SAED (JEM-2100, JEOL) were used to study the morphology and the microstructure of graphene grains and Cu hills beneath it. Raman spectra were obtained using Raman spectroscopy (LabRAM HR800) with excitation laser at 633 nm with a spot size of 1μm at room temperature.

Results and discussion

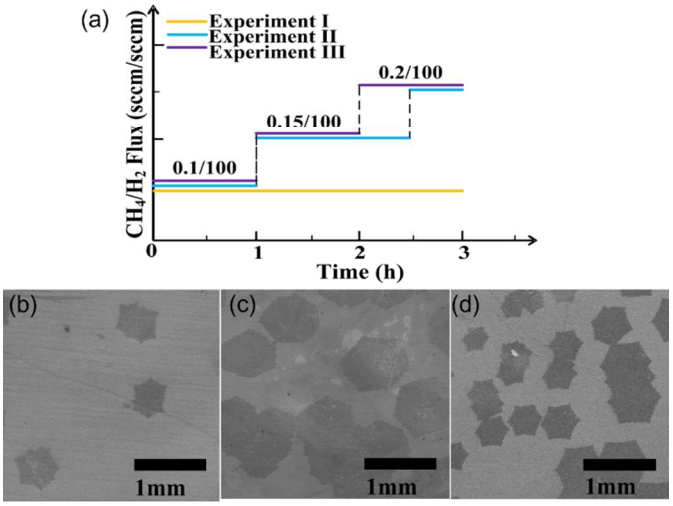

Fig. 1 (a) A chart of CH_4/H_2 flow rate during the growth experiments. SEM images of graphene grains grown on Cu foils synthesized in (b) Experiment I, (c) Experiment II and (d) Experiment III.

Fig. 1b to 1d illustrates the significantly different density and size of graphene grains grown on Cu foils in three different growth experiments. In experiment I, the flow rate of CH_4 was kept constantly at 0.1 sccm and the grain nucleation density is as low as ~0.33 mm^{-2}. The maximum grain size is about 450 μm. In such a growth rate it will take more than 5 h to obtain millimeter scale single crystal graphene grains. In the growth experiment II, the flow rate of CH_4 was stepwise increased from 0.1 sccm to 0.15 sccm and 0.2 sccm and was kept for 1, 1.5 and 0.5 h, respectively. The nucleation density increased to ~0.8 mm^{-2} and the maximum grain size increased to ~1.1 mm. Compared with experiment II, the duration of 0.2 sccm flow rate of CH_4 in experiment III was increased to 1 h. The nucleation density increased significantly to 3.88 mm^{-2}. The rapidly increased nucleation density resulted in a reduced maximum grain size of 780 μm. These results indicated that when the CH_4 flow increased from 0.1 to 0.15 sccm, the growth rate was significantly increased. While the flow rate further increased to 0.2 sccm, the nucleation density increased rapidly simultaneously. In the following part, we used the recipe in experiment II to obtain millimeter-sized graphene grains.

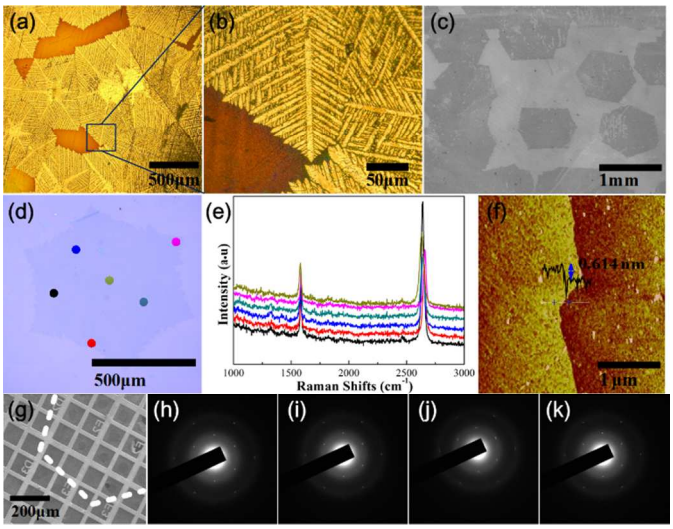

Fig. 2 (a) An optical microscopy image of a Cu foil with as-grown millimeter scale single crystal graphene grains. (b) A zoom-in optical image of the dendritic graphene grains in (a). (c) SEM image of millimeter scale graphene grains on Cu foil. (d) Optical image of a graphene domain transferred onto SiO_2/Si substrate with denoted sampling spots and (e) its six corresponding Raman spectra. (f) AFM image of graphene transferred onto SiO_2/Si. (g) SEM image of the graphene domain transferred onto a TEM grid. The edges of the domain are identified by white dashed lines. (h-k) SAED patterns taken in random windows of the TEM grid covered by the graphene domain.

After the growth, Cu foils were heated to 180℃ for oxidation treatment on a hot plate in air for 2 min to improve the optical contrast between the graphene grains and the substrate.[13] The optical image in Fig. 2a shows that the as-grown graphene grains are hexagonal in shape with dendritic structures. The multi-branched dendritic structures indicate a diffusion-limited growth kinetic in our growth condition.[8a,14] Fig. 2b is a zoom-in picture shows graphene grains with symmetric fractal structures. The graphene grains coalesce but don't overlap with each other, exhibiting highly self-limiting effect during the graphene growth.[2,10] More figures of the as-grown millimeter scale graphene grains on Cu foils are shown in Fig. 2c and Fig. S1. The largest lateral grain size is up to ~1.1 mm (edge to edge distance). The sample exhibits a fast average growth rate ~378 μm/h, which is almost comparable to that on a Pt foil,[6c] by step-wise increasing of CH_4/H_2 ratio.

Micron region Raman spectra were used to study the quality of the graphene. Fig. 2d is an optical microscopy image of a

graphene grain transferred onto a SiO_2/Si substrate. The color-coded Raman spectra corresponding to the spots marked in Fig. 2d are shown in Fig. 2e. The disorder-induced D-peak is barely visible in all of the six spectra, showing good quality of the as-grown graphene grains. Of all the six Raman spectra, the I_G/I_{2D} intensity ratios are about 0.5 and the 2D bands are symmetric and have a full width at half maximum (FWHM) about 32 cm^{-1}. These features indicate that the graphene is monolayer.[5c,8b] AFM was also employed to identify the number of the graphene layers. The height profile across the graphene domain and substrate is about 0.6 nm, corresponding to the CVD-grown monolayer graphene.[15] An SEM image of a graphene domain transferred onto a TEM grid was shown in Fig. 2g, where the edges of the domain were delineated by white dashed lines. Four SAED patterns, shown in Fig. 2h-k, were randomly taken in different windows of the TEM grid covered by the graphene domain to identify the crystallinity of the as-grown graphene domain. The four SAED patterns show the same orientation, indicating the single crystalline feature of the graphene domain.[5,14]

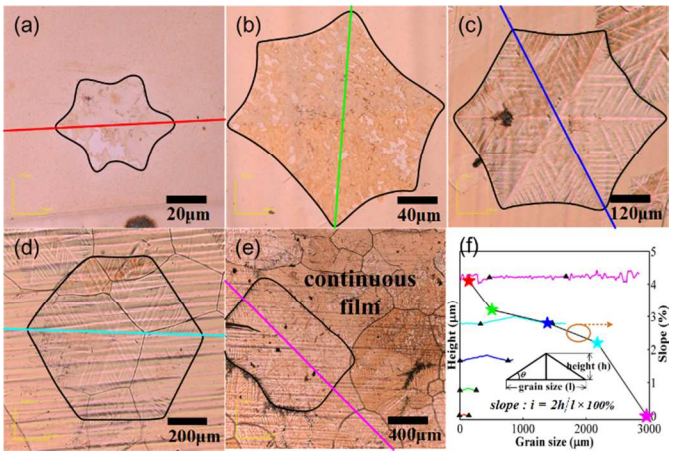

Fig. 3 (a-e) 3D laser microscopy images of the graphene grains with various grain sizes synthesized on Cu foils with different growth parameters shown in Table S1. (f) Profiles of the Cu hills beneath the graphene grains and slope of the hills as a function of the grain size corresponding to the same color line in (a-e). The inset figure depicts the definition of the slope.

Fig. 3a to 3e shows 3D laser microscopy images of the graphene grains and Cu hills with different growth parameters shown in Table S1. The profile of the Cu hills beneath the graphene grains are illustrated in Fig. 3f as cross-section contour lines. The slope of a Cu hill is defined as the ratio of the height to the grain size (half of the across-corner), shown in the inset of Fig. 3f. The slope of Cu hill is used as an index depicting the Cu hill evolution during the graphene growth. The slopes of the Cu hills are also plotted as a function of the graphene grain size in Fig. 3f. It clearly shows that the slopes of the Cu hills drop as the size of graphene grain increases. Especially when the graphene grains connect with each other, the Cu hills are almost completely flattened.

The generative mechanism of Cu hills has been well established. It is essentially a product of copper evaporation during the graphene growth. In this study, the elevated temperature is very close to the copper melting point (~1085℃). The thermal motion of the Cu atoms on the surface is also extremely active.[5b,10,16] The violent thermal motion tends to reduce the roughness of the copper surface just like what happens in thermal annealing, which is widely adopted to smooth the surface morphology.[8b,14,17] The evolution of the Cu hill is considered as a result of a competition between the copper evaporation and its thermal motion. Control experiments, conducted by running the reactors without carbon feedstock for 2h and 3h, respectively, produces no micro-scale Cu hills but smoother surface (Fig. S2). Due to the evaporation rate of the uncovered copper surface is almost constant (~4μm/h),[16] assuming that there is no thermal motion induced copper surface flattening, slope of the Cu hill beneath graphene grains will not change during graphene growth. However, the experiments tell another story. It suggests that the slope of the Cu hills decreases with the growth of the graphene grains as shown in Fig. 3f. Especially when the graphene grains merge with each other, the height of the Cu hill drops quickly shown in Fig. S3. This phenomenon confirms us that the active thermal motion of Cu atoms plays a key role in the evolution of Cu hills.

The graphene shape also evolves with the increasing grain size as illustrated by figures of Fig. 3a to 3e. The curvatures of the grain edges change from negative to nearly zero gradually when the grain size increases from 70 μm to 1.1 mm, while the dendritic feature remains. The results are different from Wu's report,[14] in which the curvature of the graphene edge was tuned continuously by changing the ratio of Ar/H_2. Because the graphene grains were synthesized in the same process condition, the shape evolution should not be attributed to a growth kinetic change. The shape evolution may be attributed to the flattening of the Cu hill as the grain size increases.

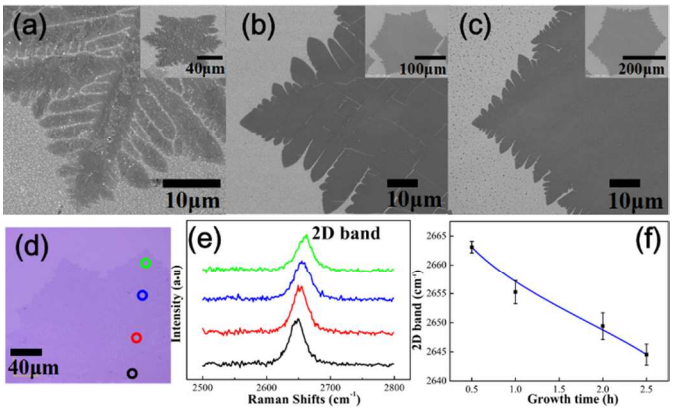

Fig. 4 SEM image of (a) a highly dendritic branch of a graphene grain shown in the inset. (b) A dendritic-to-compact branch structure of a graphene grain shown in the inset. (c) A compact branch structure of a graphene grain shown in the inset. The growth conditions are summarized in Table S2. (d) Optical microscopy image of a dendritic graphene grain transferred onto a 300nm SiO_2/Si substrate with denoted sampling spots and (e) the corresponding 2D peak of Raman spectra. (f) The position of 2D band as a function of growth time.

Here we focus on the interbranch boundaries in the dendritic structure. For dendritic graphene grains, one of the concerns is that when the growing branches merge, will they heal themselves and connect into a compact graphene lattice? High resolution SEM images of branches of graphene grains with different growth conditions (see Table S2) are shown in

Fig. 4a-c. A typically small dendritic graphene grain with remarkable inter-branch boundaries is shown in the inset of Fig. 4a. Both optical and SEM images in Fig. 2b, 4a and 4d show clear contrast with respect to the Cu substrate or SiO_2/Si substrate, indicating highly dendritic structures of the graphene branches. With longer growth time, the branches in Fig. 4b show less interbranch boundaries than Fig.4a and merge with each other partially. As the growth time increases once again, the grain boundaries heal themselves and turn into a compact graphene grain shown in Fig. 4c. It indicates that as the grains grows, the original inter-branch boundaries in the center area will be healed. More related figures are shown in Fig. S4. The healing of the interbranch boundaries gives us a positive message that we may be able to connect small graphene grains into a large one if the crystal orientation is properly controlled in a CVD process, just as Lee et al. demonstrated.[6a] The dendritic-to-compact transition mechanism lays in the stepwise increased CH_4 concentration, which leads more and more undissociated CH_4 molecules on Cu surface and results in an increased energy barrier hindering the diffusion of free C atoms. Due to the increased energy barrier, C atoms absorbed along the grain edges have enough diffusion relaxation time to find their energetically favorable location before other atoms join it. [14]

Fig. 4d is an optical image of a branch of dendritic graphene grain transferred onto SiO_2/Si substrate and Fig. 4e shows the corresponding Raman spectra. It's noted that when the sampling spots move from the center to the edge of the grain, the 2D peaks broaden and have an obvious blueshift, which is similar with the results in the other reports.[8a,18] The 2D peak shifted from 2645 cm^{-1} to 2663 cm^{-1} and the FWHM broadens from 31cm^{-1} to 34 cm^{-1} as the sampling spots move from the center to the edge of the grain. It has been proved that the physisorption of species such as water or/and oxygen will introduce a blueshift of 2D peak.[18b,19] Highly dendritic structures with more inter-branch boundaries at the edge of the grain give a higher capacity of physisorption and thus lead to a blueshift of 2D peak compared with the central compact area. The position of Raman 2D band versus growth time was plotted in Fig. 4f. The 2D band shifts towards long wavelength as growth time increases, which is consist with the situation as Raman samples from the centre to the edge of a graphene grain. The shift of 2D band provides another evidence for the improvement of the crystal quality due to the healing of the inter-branch boundaries.

Conclusions

We obtained ~1.1 mm (edge-to-edge distance) single crystal graphene grains with step-wise increased flow of CH_4. It was found that the slope of the Cu hill decreases as the graphene grain size increases. The results reveal a competition between the copper evaporation induced Cu hill building and the thermal motion induced Cu surface flattening. Most importantly, once the graphene grains merge, the Cu hill almost is completely flattened. Another important result in this report is that with a stepwise increased flow of CH_4, the interbranch boundaries in the dendritic structure are healed gradually. The blueshift of the 2D bands in Raman spectra from the center to the edge of the grain confirmed the improvement of the crystal quality due to the healing of the interbranch boundaries. It indicates a possibility that we may be able to merge small graphene grains into large ones with a proper control of the crystal orientation and growth conditions in CVD process.

Acknowledgements

The authors thank Prof. Guang Yang at International Center for Dielectric Research (ICDR), Xi'an Jiaotong University for fruitful discussions and experimental guidance. This work is financially supported by National Natural Science Foundation of China (No. 51275400, 91323303, 91123018, 61172041, 61172040) and the Fundamental Research Funds for the Central Universities.

Notes and references

[a] State Key Laboratory for Manufacturing Systems Engineering, Xi'an Jiaotong University, Xi'an 710049, China. Email: hzliu@mail.xjtu.edu.cn; Tel: +86 29-8339-9508.

[b] Vacuum Microelectronic & Microelectronic Mechanical Institute, Department of Microelectronics, Xi'an Jiaotong University, Xi'an 710049, China. Email: lwhua@mail.xjtu.edu.cn; Tel: +86 29-8266-3343.

† They contributed equally to this work.

‡ Electronic Supplementary Information (ESI) available: [details of any supplementary information available should be included here]. See DOI: 10.1039/b000000x/

1 (a) K. S. Novoselov, A. K. Geim, S. V. Morozov, D. Jiang, Y. Zhang, S. V. Dubonos, I. V. Grigorieva and A. A. Firsov, *Science*, 2004, **306**, 666; (b) Y. Zhang, Y. Tan, H. L. Stormer and P. Kim, *Nature*, 2005, **438**, 201; (c) A. K. Geim and K. S. Novoselov, *Nat. Mater.*, 2007, **6**, 183.

2 X. Li, W. Cai, J. An, S. Kim, J. Nah, D. Yang, R. Piner, A. Velamakanni, I. Jung, E. Tutuc, S. K. Banerjee, L. Colombo and R. S. Ruoff, *Science*, 2009, **324**, 1312.

3 A. W. Tsen, L. Brown, M. P. Levendorf, F. Ghahari, P. Y. Huang, R. W. Havener, C. S. Ruiz-Vargas, D. A. Muller, P. Kim and J. Park, *Science*, 2012, **336**, 1143.

4 X. Wang, L. Zhi and K. Mullen, *Nano Lett.*, 2008, **8**, 323.

5 (a) L. Gan and Z. Luo, *ACS Nano*, 2013, **7**, 9480; (b) S. Chen, H. Ji, H. Chou, Q. Li, H. Li, J. W. Suk, R. Piner, L. Liao, W. Cai and R. S. Ruoff, *Adv. Mater.*, 2013, **25**, 2062; (c) H. Zhou, W. J. Yu, L. Liu, R. Cheng, Y. Chen, X. Huang, Y. Liu, Y. Wang, Y. Huang and X. Duan, *Nat. Commun.*, 2013, **4**, 2096.

6 (a) J. H. Lee, E. K. Lee, W. J. Joo, Y. Jang, B. S. Kim, J. Y. Lim, S. H. Choi, S. J. Ahn, J. R. Ahn, M. H. Park, C. W. Yang, B. L. Choi, S. W. Hwang and D. Whang, *Science*, 2014, **344**, 286; (b) I. Vlassiouk, P. Fulvio, H. Meyer, N. Lavrik, S. Dai, P. Datskos and S. Smirnov, *Carbon*, 2013, **54**, 58; (c) L. Gao, W. Ren, H. Xu, L. Jin, Z. Wang, T. Ma, L. Ma, Z. Zhang, Q. Fu, L. Peng, X. Bao and H. Cheng, *Nat. Commun.*, 2012, **3**, 699.

7 (a) X. Li, C. W. Magnuson, A. Venugopal, J. An, J. W. Suk, B. Han, M. Borysiak, W. Cai, A. Velamakanni, Y. Zhu, L. Fu, E. M. Vogel, E. Voelkl, L. Colombo, and R. S. Ruoff, Nano Lett., 2010, 10, 4328. (b) I. Vlassiouk, M. Regmi, P. Fulvio, S. Dai, P. Datskos, G. Eres, and S. Smirnov, *ACS Nano*, 2011, **5**, 6069.

8 (a) Y. Hao, M. S. Bharathi, L. Wang, Y. Liu, H. Chen, S. Nie, X. Wang, H. Chou, C. Tan, B. Fallahazad, H. Ramanarayan, C. W. Magnuson, E. Tutuc, B. I. Yakobson, K. F. McCarty, Y. Zhang, P. Kim, J. Hone, L. Colombo and R. S. Ruoff, *Science*, 2013, **342**,720; (b) Z. Yan, J. Lin, Z. Peng, Z. Sun, Y. Zhu, L. Li, C. Xiang, E. L. Samuel, C. Kittrell, J. M. Tour, *ACS Nano*, 2012, **6**, 9110.

9 I. Vlassiouk, S. Smirnov, M. Regmi, S. P. Surwade, N. Srivastava, R. Feenstra, G. Eres, C. Parish, N. Lavrik, P. Datskos, S. Dai, and P. Fulvio, *J. Phys. Chem. C*, 2013, **117**, 18919.

10 X. Li, C. W. Magnuson, A. Venugopal, R. M. Tromp, J. B. Hannon, E. M. Vogel, L. Colombo and R. S. Ruoff, *J. Am. Chem. Soc.*, 2011, **133**, 2816.

11 T. M. Paronyan, E. M. Pigos, G. Chen and A. R. Harutyunyan, *ACS Nano*, 2011, **5**, 9619.

12 (a) Y. Xiao, H. Kim, C. Mattevi, M. Chhowalla, R. C. Maher, L. F. Cohen, *Carbon*, 2013, **6**, 7; (b) Z. Luo, Y. Lu, D. W. Singer, M. E. Berck, L. A. Somers, B. R. Goldsmith and A. T. Charlie Johnson, *Chem. Mater.*,2011, **23**,1441. (c) G. H. Han, F. Gunes, J. J. Bae, E. S. Kim, S. J. Chae, H. J. Shin, J. Y. Choi, D. Pribat, and Y. H. Lee, *Nano Lett.*, 2011, **11**, 4144.

13 (a) D. L. Duong, G. H. Han, S. M. Lee, F. Gunes, E. S. Kim, S. T. Kim, H. Kim, Q. H. Ta, K. P. So, S. J.Yoon, S. J. Chae, Y. W. Jo, M. H. Park, S. H. Chae, S. C. Lim, J. Y. Choi and Y. H. Lee, *Nature*, 2012, **490**, 235; (b) S. S. Roy and M. S. Arnold, *Adv. Funct. Mater.*, 2013, **23**, 3638.

14 B. Wu, D. Geng, Z. Xu, Y. Guo, L. Huang, Y. Xue, J. Chen, G. Yu and Y. Liu, *NPG Asia Materials*, 2013, **5**, e36.

15 H. Wang, G. Wang, P. Bao, S. Yang, W. Zhu, X. Xie, and W. Zhang, *J. Am. Chem. Soc.*, 2012, **134**, 3627.

16 A. J. Melmed and K. B. Keating, *Surf. Sci.*, 1966, **5**, 166.

17 (a) A. Mohsin, L. Liu, P. Liu, W. Deng, I. Ivanov, G. Li, O. E. Dyck, G. Duscher, J. R. Dunlap, K. Xiao and G. Gu, *ACS Nano*, 2013, **7**,8924; (b) D. Geng, B. Wu, Y. Guo, L. Huang, Y. Xue, J. Chen, G. Yu, L. Jiang, W. Hu and Y. Liu, *Proc. Natl. Acad. Sci. USA.*,2012, **109**, 7992.

18 (a) A. Das, B. Chakraborty and A. K. Sood, *Bull. Mater. Sci.*, 2008, **31**, 579; (b) A. Das, S. Pisana, B. Chakraborty, S. Piscanec, S. K. Saha, U. V. Waghmare, K. S. Novoselov, H. R. Krishnamurthy, A. K. Geim, A. C. Ferrari and A. K. Sood, *Nat. Nanotechnol.*, 2008, **3**, 210.

19 (a) Y. P. Hsieh, M. Hofmann and J. Kong, *Carbon*, 2014, **67**, 417; (b) J. Yan, Y. Zhang, P. Kim and A. Pinczuk, *Phys. Rev. Lett.*, 2007, **98**, 166802.